SECTION I - CHAPTER 3

3.1 Chapter Introduction

The work was started with two polymers [Silk Fibroin (SF) and Gellan Gum (GG)] and an antibiotic [ciprofloxacin hydrochloride (*cpr*)] as model drug. *cpr* loaded scaffolds were fabricated through freeze drying technique [Schoof et al., 2001]. We have fabricated two different types of scaffolds using SF and GG. In the first approach, the blend of both the polymers (SF-GG) was utilized to construct the scaffold. However, in second approach a double hybrid 3D scaffold of silk fibroin and gellan gum (SF-GG_b-SF) was fabricated in which drug encapsulated GG beads were entrapped between two layers of SF matrix. These two different types of scaffolds were constructed to explore that, how these both polymers behaves interactively (i.e. in SF-GG) and independently (in SF-GG_b-SF) when they coexist in a single system? *cpr* containing scaffold of pure silk fibroin (SF_{sc}), gellan gum (GG_{sc}) and beads of gellan gum (GG_b) were taken as control. First of all suitable concentrations of SF and GG were experimentally chosen for fabrication of all the types of scaffolds and bead. Thereafter, all the systems were compared for some of their basic properties like porosity, ultra structure (FESEM analysis), swelling behaviour, degradation profile and mechanical strength. Then the drug release studies were carried out in simulated wound fluid (SWF) at pH 6.0 and their drug release kinetics were investigated and compared. On the basis of basic properties and drug release behaviour; one system was selected. The selected system was further evaluated and characterized for some additional characteristics like; haemocompatibility, surface roughness, water evaporation rate antimicrobial effectivity and drug polymer interaction (FTIR analysis).

3.2 Materials

Fresh cocoons of *Bombex mori* silk worm were collected from local sericulture farm, Pilibhit, Uttar Pradesh, India. GG, lithium bromide (LiBr), sodium bi carbonate ($NaHCO_3$), sodium chloride (NaCl), calcium chloride ($CaCl_2$) and lysozyme (70,000 U/mg) were procured from Sigma–Aldrich (USA). Nutrient Broth media (NB) was used for bacterial growth whereas Nutrient Agar media (NA) media was utilized for maintaining the bacterial cultures. NA was made by supplementing 2% bacteriological agar to NB. Mueller Hinton Broth (MHB) media was utilized for cell viability test. All the ingredients of NB/NA and MHB were sourced from Hi-Media Lab. Ltd. (Mumbai, India). All the chemicals used in this study were of analytical grade and aqueous solutions and media were prepared by using double distilled deionized water. The compositions of different microbial media were as follows:

NB composition:

Media Constituent	Amount (g L^{-1})
Beef extract	1.0
Peptone	5.0
Yeast extract	2.0
NaCl	5.0
Agar	2.0
pH	7.0

MHB composition:

Media Constituent	Amount (g L^{-1})
Beef infusion	300.0
Casein hydrolysate	17.5
Starch	1.5 & pH:7.0

3.3 Methods

3.3.1 Isolation of SF from *B. mori* cocoons and fabrication of *cpr* loaded SF_{sc}

SF protein was isolated from *B. mori* silkworm cocoons through an amended standard extraction procedure (*Fig. 3.1*) [Sofia et al., 2001].

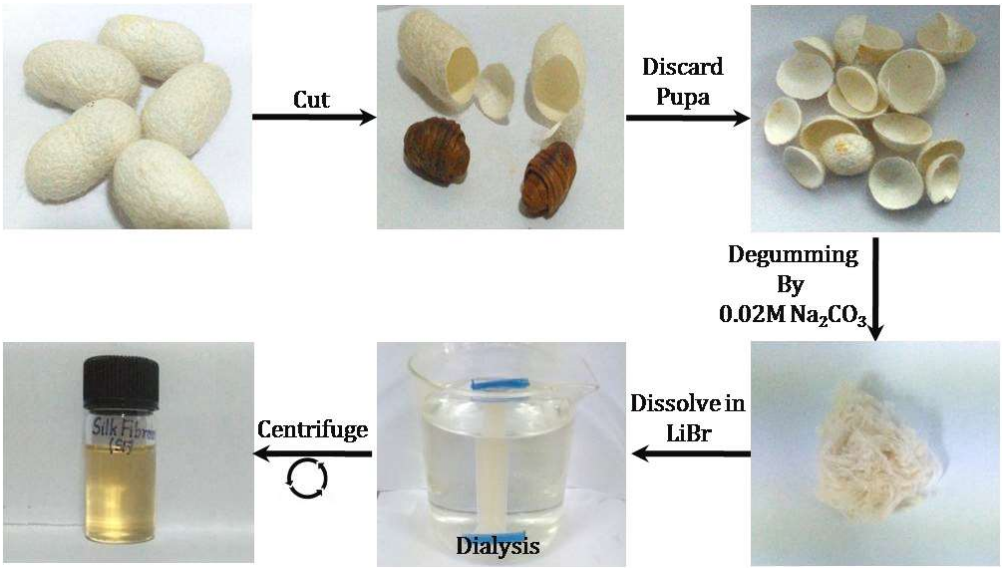

Fig. 3.1 Isolation of SF from *B. mori* cocoons

Briefly, for the isolation of SF, cocoons were first cut into small pieces and pupas were discarded. Pieces of cocoons were than boiled in 0.02 M $NaHCO_3$ for 30 min followed by washing with distilled water for degumming process to get silk fibers. Silk fibers were dissolved in 9.3 M LiBr solution to yield 8% (w/v) SF solution. Resulting solution was dialyzed against distilled water up to 3 consecutive days using dialysis membrane (MWCO 3.5 k.Da) to remove LiBr from the solution. SF concentration in dialyzed solution was determined by weighing the remaining solid mass after drying the 10 mL of SF solution at 60°C. Obtained SF solution was diluted up to 4% w/v and 1 mg/mL *cpr* was added to it. For SF_{sc} fabrication, 10 mL of SF solution was casted into glass moulds, freezed at -50°C for 6h and lyophilized using lyophilizer (LabTech, LTFD-5505). Lyophilzed/freeze dried SF_{sc} were then treated with 70% ethanol for 30 min to induce insolubility. After alcohol treatment,

scaffolds were washed with phosphate buffer saline (PBS- pH 7.4) for 15 min followed by washing with distilled water and then lyophilized again. All the washing solutions were collected for analysis of leached drug during processing.

3.3.2 Preparation of *cpr* loaded GG_b beads and GG_{sc} scaffolds

GG solution was prepared by dissolving GG (1.5 % w/v) in double distilled deionized water at 90°C. The obtained clear solution of GG was then cooled down up to 50°C and *cpr* (1 mg/mL) was dissolved in to this solution. The resulting solution was utilized to construct the *cpr* loaded GG_b and GG_{sc}. The GG_b were prepared by dripping *cpr*-GG solution into 100 ml of 0.5 M $CaCl_2$ using a 10 mL syringe. $CaCl_2$ was kept under starring during dripping *cpr*-GG solution. Constructed beads were sieved and lyophilized after washing wish distilled water.

For construction of GG_{sc}, 10 mL of *cpr* containing GG solution was casted into glass moulds and allowed to solidify by cooling down at room temperature. Solidified GG was then treated with 100 mL of 0.5 M $CaCl_2$ solution for gelation and to induce cross linking within gel matrix [Rodri´guez-Hernandez et al., 2003]. After gelation, the resulted GG hydrogel was freezed at -50°C for 6h and thereafter lyophilized to obtain freeze dried GG_{sc}.

3.3.3 Preparation of SF-GG and SF-GG_b-SF scaffolds

SF-GG scaffold was constructed by freeze drying of *cpr* (1 mg/mL) containing 10 mL blended solution of 4% SF and 1.5 % GG in the equal ratio. After freezing the blend solution (at -50°C for 2h) in to the moulds; it was gelated with $CaCl_2$ (0.5 M) for 10 min and subsequently freezed and then lyophilized. Freeze dried scaffolds were first treated with 70% ethanol for 30 min and then treated with PBS (15 min) followed by washing with distilled water and re-lyophilized.

SF-GG_b-SF double hybrid 3D scaffold was prepared by hybridizing both the systems together *viz.* SF and GG_b. For SF-GG_b-SF preparation, *cpr* (1 mg/mL)

containing, 10 mL solution of SF (4% w/v) was poured into glass mould. The poured SF was frozen by keeping this solution at -50°C for 2 h. After freezing, a single layer of GG_b was placed on top of the frozen SF. Further, on top of placed GG_b layer; another layer of SF (4% w/v) solution was again poured and whole system was frozen at -50°C for 6 h followed by lyophilization. Constructed SF-GG_b-SF scaffolds were treated with 70% (v/v) ethanol for 30 min, washed with PBS (pH 7.4) as well as by distilled water and then again freeze dried. *Fig. 2 a-e* represents the schematic diagram for fabrication procedure of all types of scaffolds and bead used in this study.

3.3.4 Scanning electron microscopy and measurement of scaffold porosity

The ultra-structure of the scaffolds was observed with Zeiss Evo-18 field emission scanning electron microscope (FESEM). Polymeric scaffolds were cut into thin slice of 0.5 cm^2 and specimens and sputter coated with gold before analysis. Elemental composition of associated FESEM image was studied through energy dispersive X-ray spectroscopy (EDX). EDX detector was associated with FESEM.

Porosity of scaffolds was calculated by the liquid displacement method [Nazarov et al., 2004]. For porosity measurement, the scaffold was first submerged in a known volume of hexane (V_1) in a graduated cylinder. After 5 min, total volume of hexane and the hexane-impregnated scaffold was recorded as V_2. When the liquid-impregnated scaffold is removed, the remaining liquid volume was considered as V_3. The porosity of the scaffold (ε) was calculated by using following equation:

$$\%\varepsilon = \frac{V_1 - V_3}{V_2 - V_3} \times 100$$

Where $V_1 - V_3$ represent the volume of hexane within the scaffold whereas $V_2 - V_3$ denotes the total volume of the scaffold.

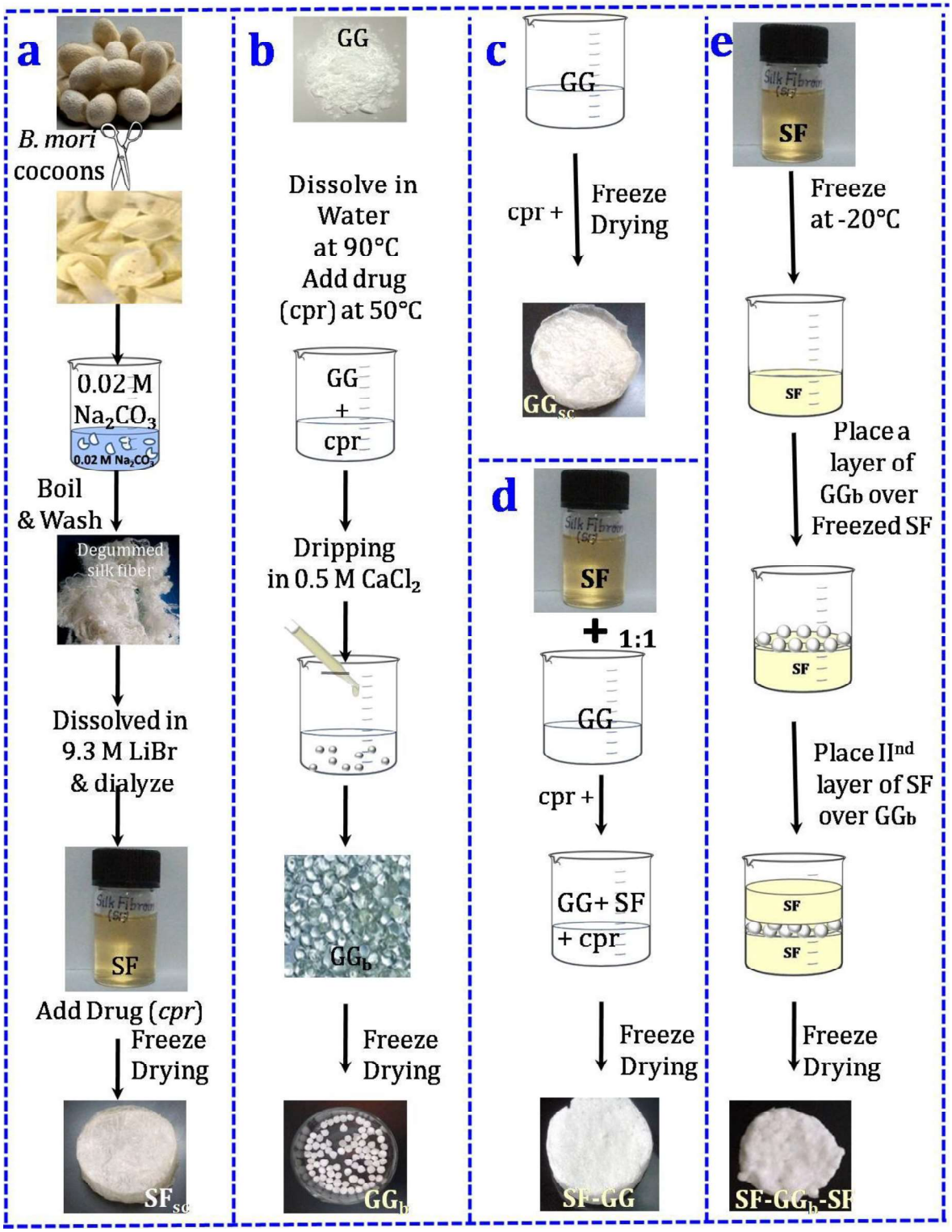

Fig. 3.2 Schematic diagram for fabrication procedure of SF_{sc}, GG_b, GG_{sc}, SF-GG and SF-GG_b-SF.

3.3.5 Drug loading and release study

The amount of loaded drug into the scaffolds and in beads was calculated from difference between the total antibiotic added and the amount leached out in washing solutions. Drug loading efficiency of different scaffolds (SF_{sc}, GG_{sc}, SF-GG, SF- GG_b-SF) and in GG_b was calculated by using following equation:

$$Drug\ loading\ efficiency\ \% = \frac{Total\ antibiotic\ added - Antibiotic\ \ washing\ solution}{Total\ antibiotic\ added} \times 100$$

Drug release studies were carried out in Simulated Wound Fluid (SWF) at pH 6.0 because the pH of chronic wounds has been reported to be slightly acidic and SWF is isotonic with the fluid present at wound site [Porstmann, 1989]. SWF was prepared by dissolving 8.30 g NaCl and 0.28 g $CaCl_2$ to 1 L of distilled deionized water which is equivalent to 142 mM NaCl (aq) and 2.5 mM $CaCl_2$ (aq) [Andrew, 2011]. For release studies, equal weights (50 mg) of scaffolds (SF_{sc}, GG_{sc}, SF-GG, SF-GG_b-SF) and GG_b were kept in to 50 mL of SWF to maintain the weight and volume ratio of 1 mg/mL. All the flasks were incubated at 37°C and 50 rpm in incubator shaker. Samples of 2 mL volume were withdrawn at regular time intervals and equal amount of fresh SWF was added to flasks for maintaining the volume of release medium constant. Released amount of *cpr* was assayed in the sample to estimate the cumulative percentage release.

3.3.6 Drug assay

The *cpr* assay was performed by method as reported by Wang et al [Wang et al., 2007]. Concentration of released *cpr* in the samples was assayed in triplicate using UV–visible spectrophotometer (Evolution 201, Thermo Scientific) at 277 nm and mean value was taken in account. Before evaluating the samples, the standard curve was plotted as given in *Fig 3.3.*

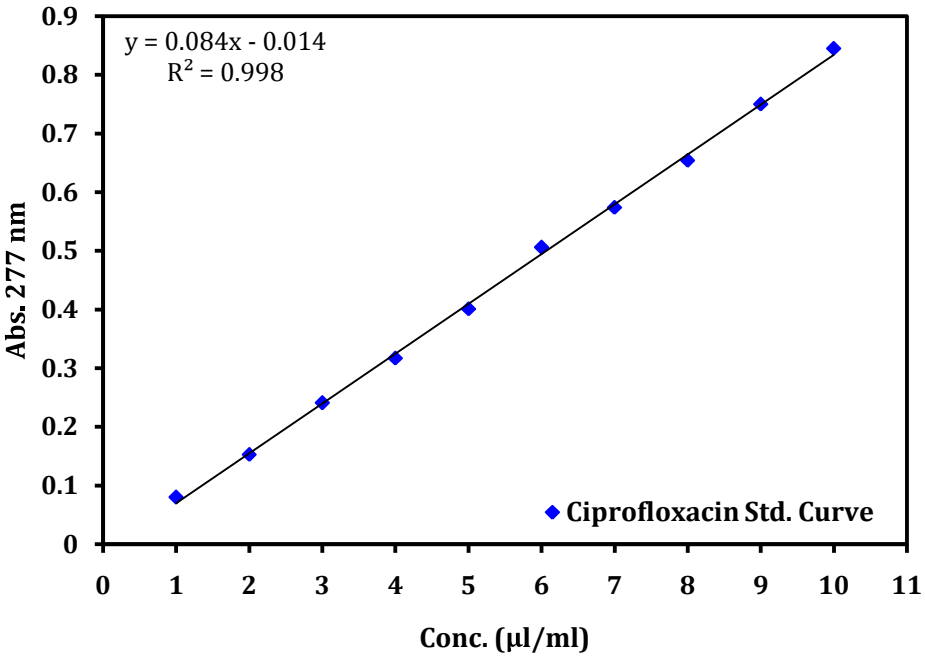

Fig 3.3 Standard curve of ciprofloxacin hydrochloride (*cpr*)

3.3.7 Drug release kinetics

The drug released kinetics of *cpr* from SF_{sc}, GG_{sc}, GG_b, SF-GG and SF-GG_b-SF was analyzed via fitting the in-vitro release data with zero order (eq. 1), first order (eq. 2), Higuchi (eq. 3) and Korsmeyer-Peppas (eq. 4) mathematical models to investigate the mechanism of drug release [Costa and Lobo 2001].

$$Q_t = Q_0 + K_0 t \quad \text{[eq. 1]}$$

$$Log\ Q_t = Log Q_0 - kt/2.303 \quad \text{[eq. 2]}$$

$$Q_t = kt^{1/2} \quad \text{[eq. 3]}$$

$$Q_t = kt^n \quad \text{[eq. 4]}$$

Where 'Q_t' is amount of drug released in solution at time t; 'Q_0' is initial amount of drug in the solution; 'k' is release constant; 'n' is release exponent of the reaction and 't' denotes time. The regression coefficient (R^2) was considered as the base for prediction of best fitting model to the system.

3.3.8 Swelling studies

Swelling behavior of all the systems (SF_{sc}, GG_{sc}, GG_b, SF-GG and SF-GG_b-SF) was evaluated through swelling studies conducted in both SWF (pH 6.0) and water (pH 7.0). For swelling study, 100 mg of scaffolds/bead were weighed and then separately immersed in 100 mL of SWF and water subsequently incubated at 37°C. After regular time interval, swollen scaffolds/bead were removed and gently wiped with tissue paper for absorbing the excess of solution and then weighed. The degree of swelling was calculated as swelling ratio (SR) with the help of following equation:

$$SR = \frac{(W_s - W_d)}{W_d}$$

Where, 'W_s' and 'W_d' are corresponding to the mass of swollen and dry scaffolds/bead respectively.

3.3.9 In-vitro degradation studies

In-vitro degradability of all the scaffolds and beads (SF_{sc}, GG_{sc}, GG_b, SF-GG, SF-GG_b-SF, GG_b) was investigated out up to 28 days in SWF (pH 6.0) containing 1.6 µg/mL (i.e. 112 U/mL) of lysozyme from egg white. lysozyme concentration was chosen on the basis of literature which reports that wounds contain average lysozyme concentration of 112 U/mL [Porstmann, 1989]. Degradation experiments were carried out with 1 mg/mL initial weight of scaffolds/bead in SWF incubated at 37°C in sterile conditions. SWF was replaced each day to ensure the continuous enzymatic activity. After definite time of incubation, the scaffolds/bead was carefully withdrawn and freeze-dried after washing with distilled water. The extent of in vitro degradation was calculated as the percentage of weight change of the dry scaffolds/bead before and after incubation.

3.3.10 Mechanical properties

Mechanical properties of SF_{sc}, GG_{sc}, GG_b, SF-GG and SF-GG_b-SF were evaluated through universal testing machine (UTM, Instron, 3369) in compression mode with a 10 N of load cell. Mechanical behavior of the scaffolds was monitored up to 75% of compression with crosshead speed 1 mm/min. The initial slope of the linear section of the stress–strain curve represents the compressive modulus whereas ultimate compressive strength was calculated by determining the cross point of stress-strain curve via line drawn at parallel to strain axis at 75% strain [Thomson et al., 1998].

3.3.11 Selection of best system and post selection evaluation

All the systems under study were compared for their above studied properties and most appropriate system was selected. The selected system was further evaluated for its haemocompatibility, surface roughness, water evaporation rate, antimicrobial effectivity and drug polymer interaction. These mentioned properties were evaluated through haemcompatibility assay, atomic force microscopy, dehydration test, cell viability test and fourier transform infrared (FTIR) spectroscopy, respectively. FTIR analysis was performed using FTIR spectrophotometer (Varian-3100) to screen the functional groups present on selected scaffold and their interaction with drug *cpr*. IR spectra of SF, GG_b, and *cpr* were taken as control for compare. The IR spectra were collected in the in the range of 4000–400 cm^{-1}.

Haemocompatibility is one of the parameter that ensures the biocompatibility and usability of the material for its biomedical applications. The haemcompatibility assay was performed according to standard procedure with minor amendments [Mehta et al., 2014]. For the assay, fresh human blood was collected from healthy volunteer in anticoagulant coated vials. The selected scaffold was cut into small pieces of 1 cm × 1cm × 0.5 cm without sharp edges. Before test

the scaffold samples were equilibrated in physiological saline for 30 min at 37° C. Thereafter the equilibrated pieces of scaffold were transferred to 10 mL of physiological saline solutions containing 2% of whole blood inoculum. The system was then incubated at 37° C for 1h. After incubation, the test solutions were centrifuged at 5000 rpm for 5 min and supernatant was collected for optical density measurement at 540 nm. Distilled water with 2% of blood (showing 100% hemolysis) and 0.9% saline with 2% of blood (showing 0% hemolysis) served as positive and negative controls, respectively. The percentage hemolysis was calculated according to given equation:

$$\%\, Hemolysis = \frac{(O.D)Test\ solution - (O.D)Negative\ control}{(O.D)Possitive\ control - (O.D)Negative\ control}$$

It is already reported by many research groups that rough surfaces are more suitable for the cell attachment, migration and proliferation as compare to smooth surfaces [Lampin, et al., 1997]. Therefore the surface roughness of selected system was ensured through AFM analysis (Dimension Edge, AFM-Bruker) using NT-MDT working in the contact mode. Screening areas was randomly selected over the sample and analyzed. AFM images have been processed using 'NANOSCOPE' software.

WER for the selected scaffold was measured to evaluate the dehydration rate and moisture permeability [Li et al., 2015]. For WER measurement the selected scaffold was first cut into a cube piece with dimensions 1 cm × 1 cm × 1 cm and then emerged into SWF for 3h to ensure the swelling equilibrium. Thereafter swelled piece of scaffold was kept in an incubator at 37°C and 35% relative humidity. The weight loss with proceeding of time was recorded at regular time intervals and WER was calculated using following equation:

$$\text{WER or \% Weight Loss} = \frac{W_t}{W_i} \times 100$$

Where W_i is the initial weight of swelled scaffold and W_t is the weight of scaffold after time interval of 't'.

Time dependent antibacterial behavior of released *cpr* from selected scaffold was determined through cell viability test on Gram negative bacteria *Eischherichia coli* (*E. coli,* MTCC 1680) and Gram positive bacteria *Staphylococcus aureus* (*S. aureus,* MTCC 9886). Bacterial strains were procured from Microbial Type Culture Collection and Gene Bank (MTCC), Chandigarh, India. Bacterial cultures were preserved on the slants of NA. The inoculums were prepared by transferring a single bacterial colony from NA slant into 50 mL of MHB with a sterile loop. Inoculated MHB was incubated overnight at 37°C at shaking speed of 100 rpm. After bacterial growth, the optical densities of the resultant microbial culture suspensions were adjusted to 0.5 McFarland standard (0.5 mL of 0.048 M $BaCl_2$ in 99.5 mL of 0.18M H_2SO_4) by adding sterile MHB broth to achieve bacterial density of 10^7 CFU/mL [Petrus et al., 2011]. 50 mg of drug loaded sample of selected scaffold was transferred to 50 mL of prepared inoculums of MHB and systems were incubated at 37°C. Samples (100 µL) were withdrawn at regular time interval of 1 h and than 10 fold diluted. The diluted samples were separately spread onto MHA plates and incubated at 37°C for 24 h. MHA plate inoculated with pure inoculums were used as control. After incubation, colonies were counted on plates and their number was compared with control plate to calculate the percentage viability of cells.

3.4 Results and discussion

3.4.1 Morphology, ultra-structure and porosity of scaffolds

Two hybrid scaffolds of silk fibroin and gellan gum *viz.* SF-GG (blend) and SF-GG_b-SF (3D hybrid scaffold) and three control scaffolds/beads viz. SF_{sc}, GG_{sc} and GG_b

were fabricated through freeze drying method. All the systems were preloaded with *cpr* drug. External morphology, corresponding FESEM images and associated EDX spectra of SF_{sc}, GG_{sc}, SF-GG, GG_b and SF-GG_b-SF are shown in *Fig 3.4 (a-i)* and *Fig. 3.5 (a-f).* Average diameter of GG_b was approximately 2.0 ± 0.5 mm whereas the average diameter and height of all scaffolds were 4.5 ± 0.3 cm and 0.7 ± 0.2 cm respectively. Comparative FESEM analysis showed the variability in surface architecture and porosity for different scaffolds in this study. It was observed that surface was less porous in case of gellan gum systems (GG_b and GG_{sc}) and in blend scaffold (SF-GG).

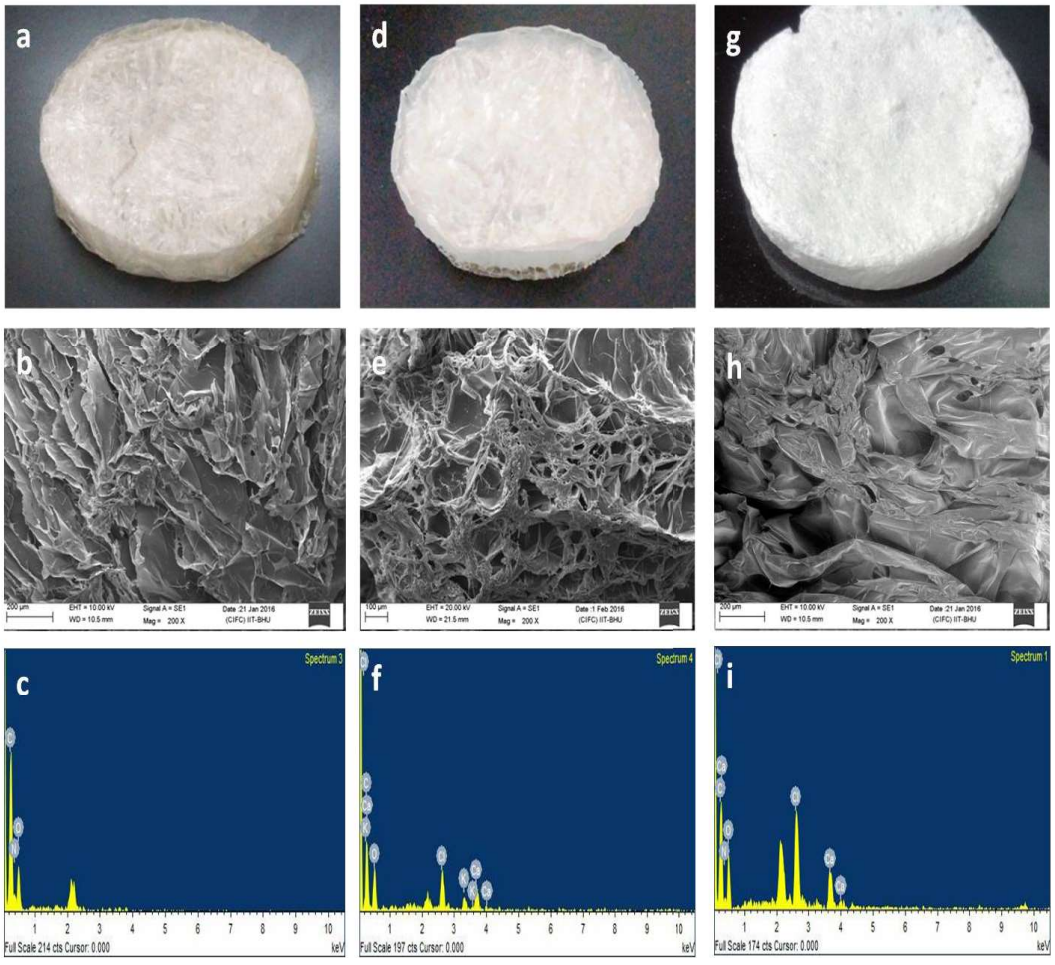

Fig. 3.4 Morphology of different scaffolds/beads, their corresponding FESEM images showing ultra-structure and EDX spectra showing elemental profile respectively: (a, b, c) SF_{sc}, FESEM image and EDX spectra (d, e, f) GG_{sc}, FESEM image and EDX spectra (g, h, i) SF-GG, FESEM image and EDX spectra.

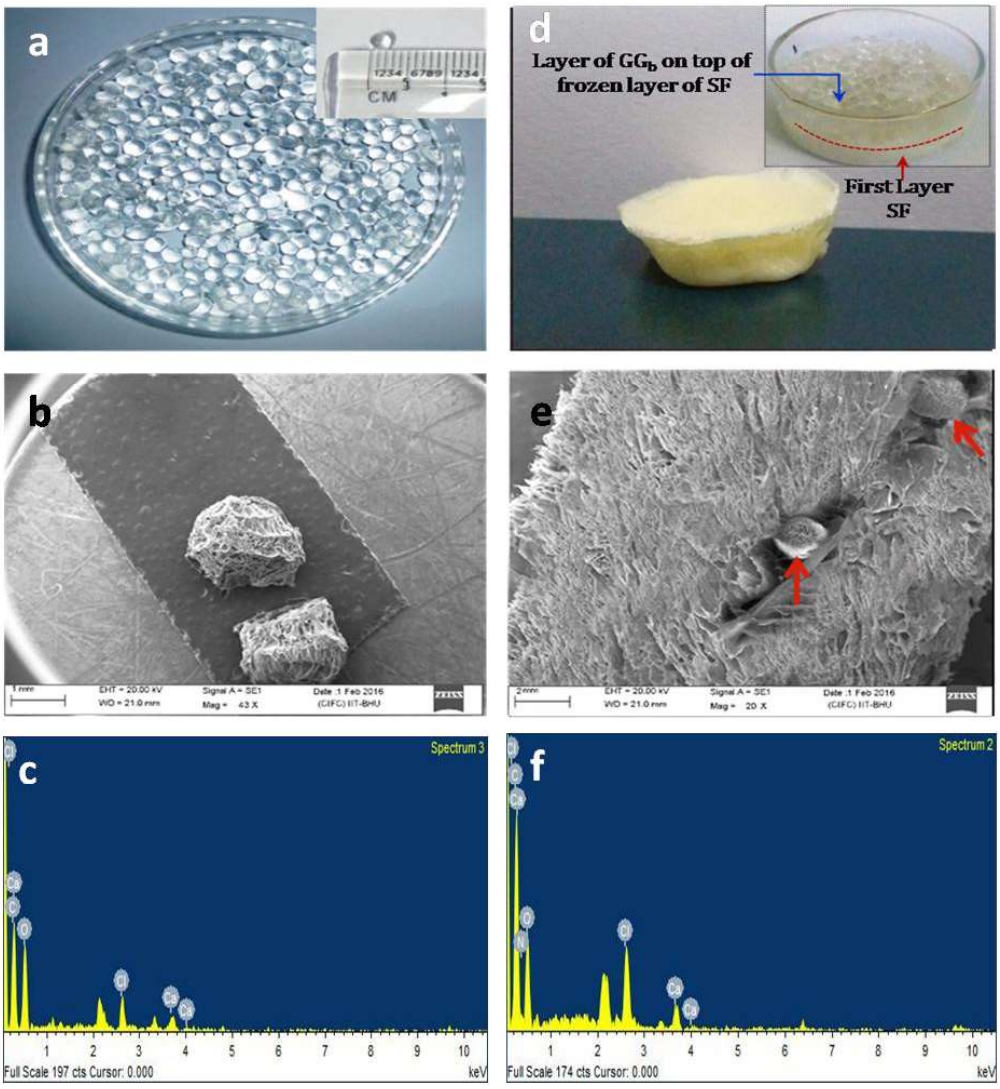

Fig. 3.5 Morphology, corresponding FESEM images and EDX spectra of GG_b (a, b, c) and of SF-GG_{sc}-SF (d, e, f).

This observation was also supported by the results of porosity measurement through liquid displacement method (*Table 3.1*). SF_{sc} was found maximum porous (87.5%) while porosity was minimum (42.3%) in the case of GG_b. Blending of GG with SF, deplete the porosity by ~16% as compare to SF_{sc}, whereas entrapment of GG_b in SF matrix reduces the porosity just by 3%. As per the various scientific reports; gellan gum undergoes ionic gelation in the presence of various cations

[Morries et al., 2000]. During gelation, random coil chains of gellan gum forms double helical junctions followed by aggregation of double helical segments to form a 3D network by complexation with cations and hydrogen bonding with water [Grasdalen et al., 1987]. This is known as coil-to-helix transition mechanism for gelation of gellan gum. The high viscosity and highly interwoven network of gellan gum may leads to lesser porosity of GG_{sc}, GG_b and blended system SF-GG. Whereas, SF-GG_b-SF 3D hybrid scaffold do not exhibit so drastic depletion in porosity because in this system both the polymers (SF & GG) have separate entity.

Table 3.1 Percentage porosity of SF_{sc}, GG_{sc}, GG_b, SF-GG, and SF-GG_b-SF calculated through liquid displacement method

Name of the system	% Porosity
SF_{sc}	87.5
GG_{sc}	61.0
GG_b	42.3
SF-GG	71.5
SF-GG_b-SF	84.5

3.4.2 Drug loading and release studies

Drug (*cpr*) loading efficiencies of all the systems under study were evaluated and the results are shown in *Fig 3.6.* Loading efficiency of *cpr* was found to be minimum (2.3%) in case of SF_{sc} whereas it was maximum (4.0%) in case of GG_b. GG_{sc}, SF-GG and SF-GG_b-SF 3D hybrid scaffold showed intermediate *cpr* loading efficiencies 3.8%, 3.1% and 3.7% respectively. As reported by some researchers that increase in the viscosity of polymeric system enhances the entrapment efficiencies of drugs [Rangaraj et al., 2010; Oya et al., 2007]. Thus, this might be the reason

associated with the higher *cpr* loading efficiency of viscous GG as compare to SF. Moreover, GG_b holds slightly higher amount of *cpr* than that of GG_{sc}. This is because in the form of scaffold, gellan gum matrix is more porous as compare to in the form of beads hence more surface area is exposed for drug leaching in the case of GG_{sc} leading to lower *cpr* loading efficiency.

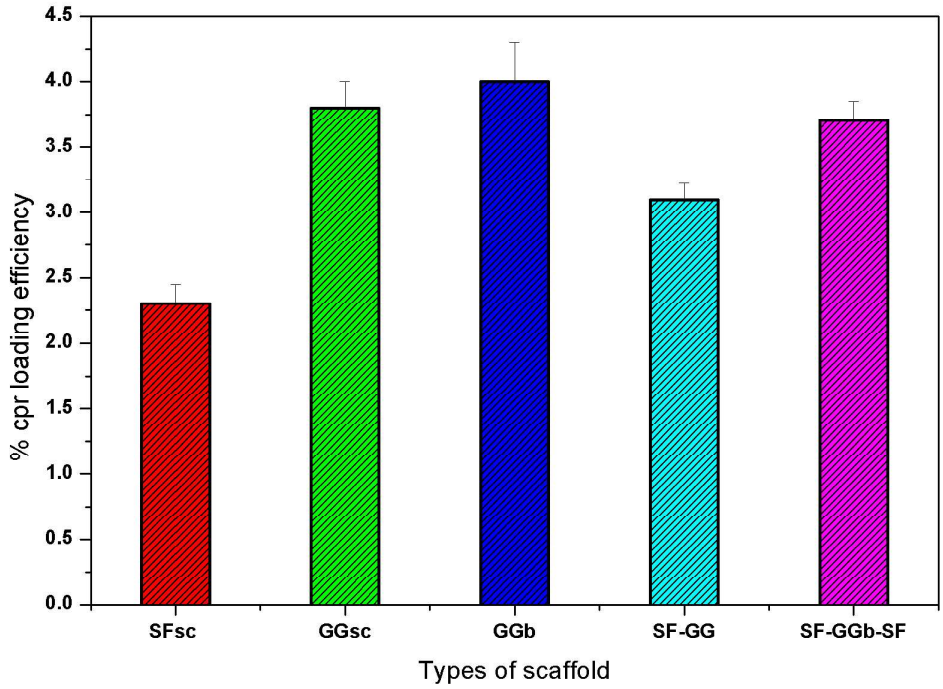

Fig. 3.6 Percentage loading efficiency of *cpr* in different scaffolds/beads

After loading studies the *cpr* release studies were carried out in SWF at pH 6.0 and the results are shown in *Fig. 3.7.* It is clear from the results that all the systems exhibited an initial bust release. This initial *cpr* release rate was rapid in case of GG_{sc} and GG_b as compare to SF_{sc}. GG_{sc} and GG_b were found to release ~100% of incorporated drug in first 5h whereas SF_{sc} releases 79.5% of loaded drug in 14h. SF-GG and SF-GG_b-SF illustrated the intermediate release pattern between SF_{sc} and GG_{sc}/GG_b. As it is well known that, drug release from hydrophilic natural polymers is governed by various complex interactions between its swelling, erosion and diffusion behavior [Osmałek et al., 2014, Ferrero et al., 2010]. Therefore it can be

concluded that grater hydrophilicity of GG results to faster release of *cpr* from matrix whereas lesser hydrophilic nature of SF hinders the water to penetrate in matrix thus resulted into more sustained release of *cpr* due to poor solvent diffusibility. Moreover, *cpr* releases from SF-GG_b-SF in a more sustained manner as compared to SF-GG which could also be governed by relative hydrophilicity and swelling index of both the systems. Furthermore, in case of SF-GG_b-SF, *cpr* have to cross two barriers before it get released from entrapped gellan gum beads. The first barrier of gellan gum bead and another barrier of covering silk fibroin which leads to more sustained release of *cpr* than that of from SF-GG.

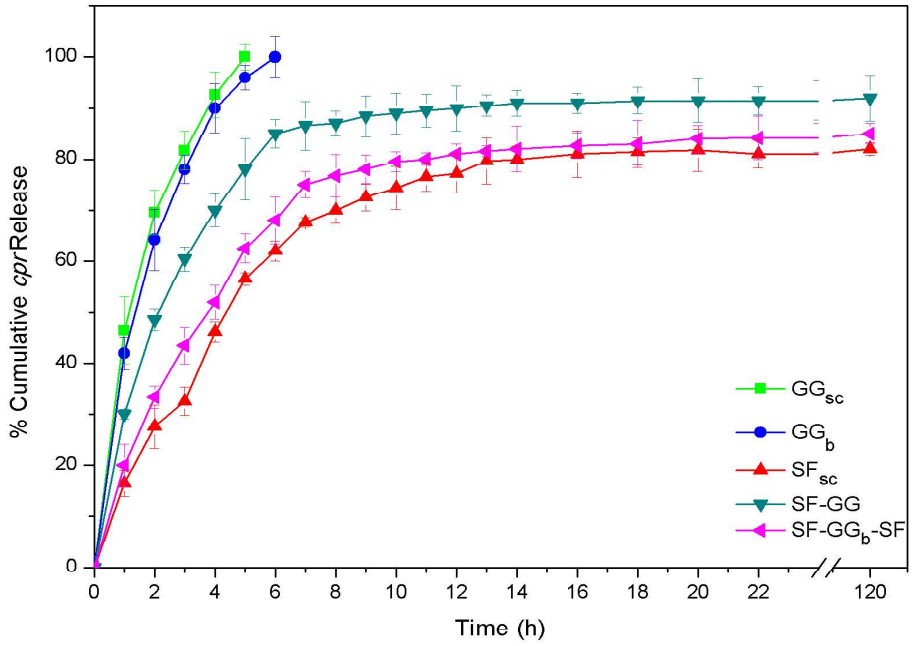

Fig 3.7 Cumulative *cpr* release from different scaffolds/beads viz. SF_{sc}, GG_b, GG_{sc}, SF-GG & SF-GG_b-SF at pH 6.0 in SWF

3.4.3 Drug release kinetics and *cpr* release mechanism

Drug release kinetics was studied and release mechanism of *cpr* was predicted through data fitting with in-vitro release kinetic models viz. zero order, first order, Higuchi and Korsmeyer-Peppas model. Obtained kinetic parameters for all the systems have enlisted in *Table 3.2.*

Table 2. Kinetic parameters for cpr release from SF_{sc}, GG_{sc}, GG_b, SF-GG, and SF-GG_b-SF

Kinetic Model	Parameter	System				
		SF_{sc}	**GG_{sc}**	**GG_b**	**SF/GG**	**SF-GG_b-SF**
Zero order	k	20.31	9.321	8.865	11.92	8.304
	R^2	0.835	0.535	0.659	0.506	0.835
First order	k	0.067	0.035	0.044	0.041	0.050
	R^2	0.908	0.727	0.686	0.708	0.800
Higuchi	k	43.30	28.5	28.89	29.56	26.13
	R^2	0.970	0.950	0.943	0.895	0.962
Korsmeyer-Peppas	n	0.458	0.508	0.646	0.482	0.693
	k	0.990	29.57	20.84	35.64	17.27
	R^2	0.983	0.944	0.930	0.932	0.976

It is evident from the results that release kinetics *cpr* from SF-GG and SF-GG_b-SF was best fitted with Korsmeyer-Peppas model. Regression coefficient (R^2) and release exponent (n) were 0.976 and 0.693 for SF-GG_b-SF, whereas were 0.932 and 0.482 for SF-GG. In both the cases the values of release exponents were; $0.45<n<0.89$ which indicates that *cpr* mainly released through anomalous (non-Fickian) diffusion and the whole release process is together governed by swelling, gel formation, diffusion and degradation of polymeric matrix [Costa 2001, Singhvi and Singh; 2011]. SF_{sc}, GG_b and GG_{sc} also showed best fitting with Korsmeyer-Peppas model thus showed similar release mechanism. Moreover, regression coefficients (R^2) of SF_{sc}, GG_b, GG_{sc}, SF-GG and SF-GG_b-SF are also in good agreement with Higuchi

kinetic model which indicated that some portion of the drug also release through Fickian diffusion [Desai et al., 1966].

3.4.4 Swelling Studies

Swelling study was carried out in SWF to investigate the capacity of absorption of exudates. The results for all the systems have shown in *Fig. 3.8.* GG_{sc} and GG_b were found to have greater swelling ratios 22.7 and 20.5 respectively, as compare to SF_{sc}, which showed comparatively lesser swelling ratio i.e. 8.5. This was due to the superior hydrophilicity of GG over SF. Blending of GG with SF improved the swelling properties of SF. SF-GG_b-SF also showed improved swelling properties over SF_{sc} due to entrapped GG_b in SF matrix. But SF-GG_b-SF showed lesser degree of swelling ratio as compare to SF-GG because in SF-GG_b-SF the hydrophilic GG component was masked by two layers of SF and was not much exposed for aqueous medium. Therefore by blending and by bead entrapment the swelling properties of scaffolds can be tuned according to need.

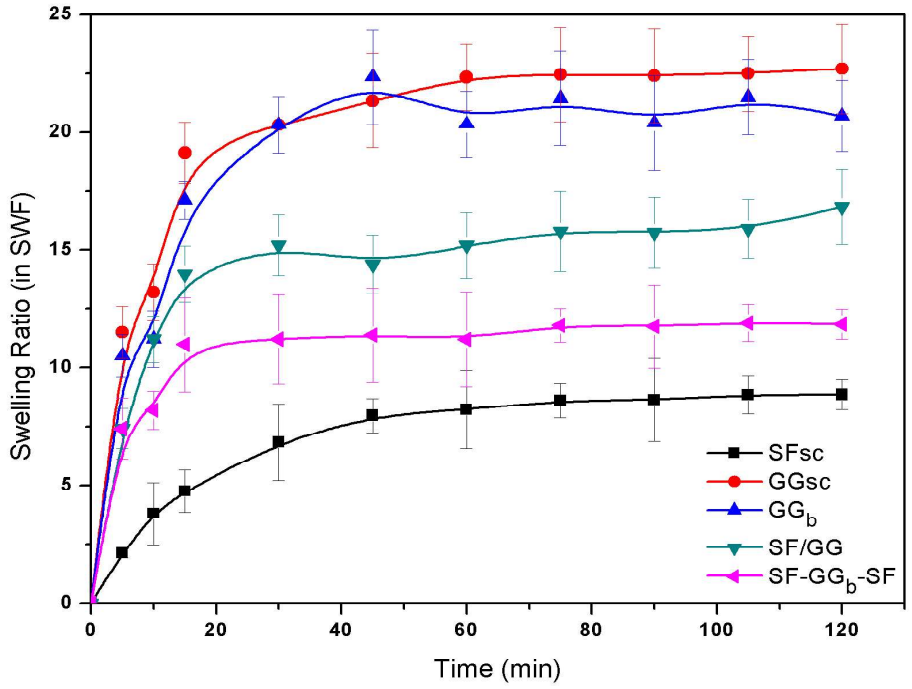

Fig. 3.8 Swelling ratio of different scaffolds/beads viz. SF_{sc}, GG_b, GG_{sc}, SF-GG & SF-GG_b-SF at pH 6.0 in SWF

3.4.5 Mechanical properties

Fig 3.9 represents the mechanical behavior of scaffolds in terms of strain created at applied stress (load). The ultimate compressive strength at 75% compression and compressive modulus at 2% of initial strain for all the systems are shown in *Fig. 3.10* and *Fig. 3.11* respectively. SF_{sc} was found to have maximum compressive strength (0.67 MPa) and compressive modulus (0.011 MPa). The values of compressive strength and compressive modulus for SF-GG_b-SF were 0.64 MPa and 0.0108 MPa respectively which were very close to the compressive strength and compressive modulus of SF_{sc}, this was due to predominant silk fibroin matrix in SF-GG_b-SF. Compressive strength and compressive modulus of SF-GG were found to be significantly decreased as compared with SF_{sc} which may be due to the altered native matrix architecture of the individual polymers in blend system.

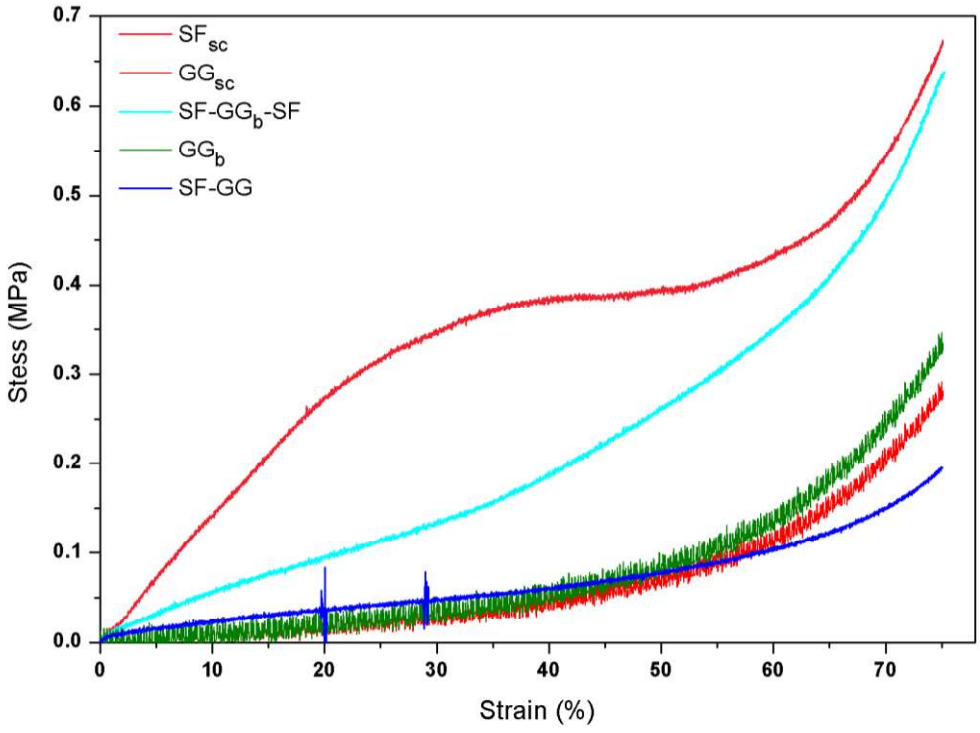

Fig 3.9 Stress *vs* strain curve for SF_{sc}, GG_b, GG_{sc}, SF-GG & SF-GG_b-SF up to 75% of compression

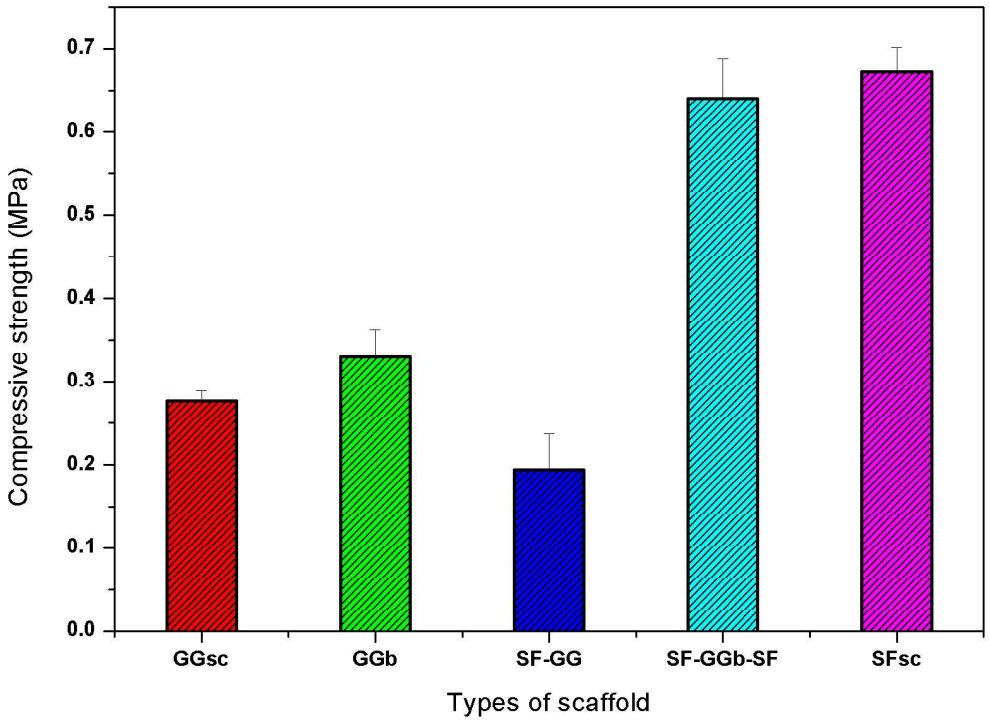

Fig 3.10 Ultimate compressive strength of SF_{sc}, GG_b, GG_{sc}, SF-GG & SF-GG_b-SF at 75% of compression; calculated from stress strain curve

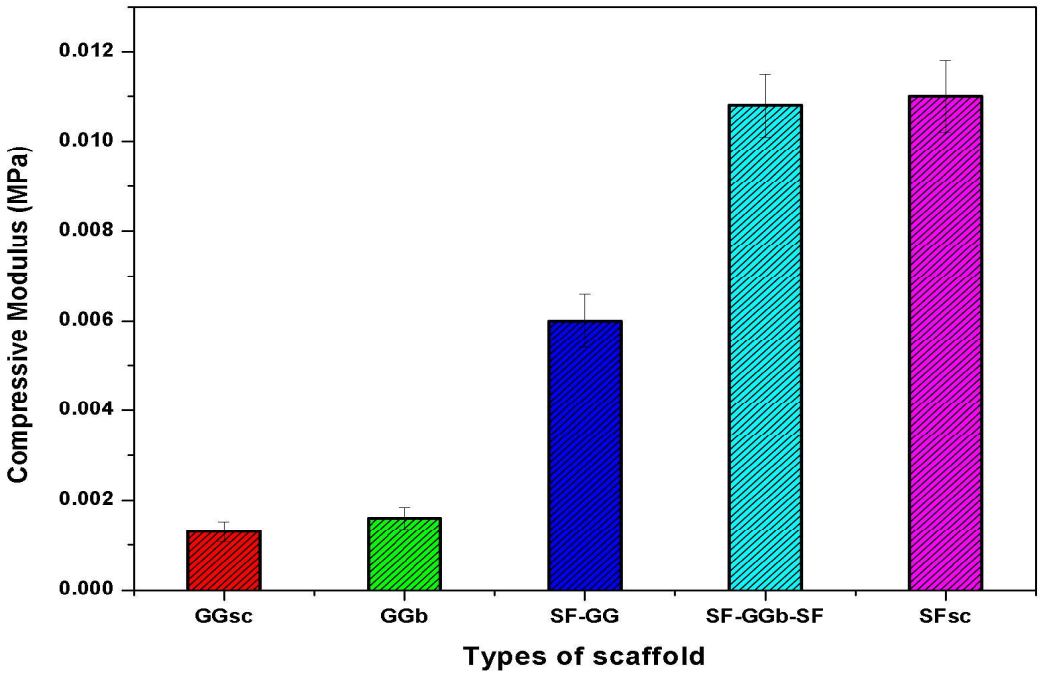

Fig 3.11Compressive modulus of SF_{sc}, GG_b, GG_{sc}, SF-GG & SF-GG_b-SF at initial 2% strain

3.4.6 Degradation Studies

Degradation studies were performed in SWF at pH 6.0 containing lysozyme (112 U/mL). Degradation was monitored up to 28 days. Results showed very minor degradation in each case. SF_{sc}, GG_b, GG_{sc}, SF-GG and SF-GG_b-SF were found to degrade by 4.0±2.2, 5.4±2.6, 6.2±1.6, 4.4±2.1 and 4.7± 2.9% respectively. This little loss in weight signifies that both the polymers are not being attacked by lysozyme present in SWF due do absence of attacking site for the enzyme action. This is worthy to note here that silk fibroin is well reported as slowly biodegradable polymer and it takes nearly 2 years to completely degrade in in-vivo system by body protease produced as foreign body response [Anderson et al., 2006].

3.4.7 Selection of best system and post selection evaluation

Morphology and porosity, mechanical properties, swelling behavior, degradation properties and drug release behavior of all the studied systems were mutually compared on the basis their relative performance. The performance was graded on a five star comparative grade scale and the SF-GG_b-SF was selected as best system on the basis of overall score. Comparison table is given as *Table 3.3.*

Table 3.3 Comparison table for the selection of best scaffold among SF_{sc}, GG_b, GG_{sc}, SF-GG and SF-GG_b-SF

Types of Scaffold	Properties				
	Porosity	Swelling properties	Mechanical Strength	Drug release Properties	Degradation
SF_{sc}	*****	*	*****	*****	*
GG_{sc}	**	*****	**	*	***
GG_b	*	*****	**	**	***
SF-GG	***	***	***	***	**
SF-GG_b-SF	****	****	****	****	**

3.4.8 Some further characterizations of selected scaffold to explore its suitability for biomedical applications

a. Haemocompatibility

Haemocompatibility of SF-GG_b-SF was determined by determining percentage hemolysis. The results are shown in *Fig. 3.14.* In the hemolysis test SF-GG_b-SF showed 3.7% hemolysis. Because the selected scaffolds exhibited less than 5% of hemolysis, hence SF-GG_b-SF can be considered as highly haemocompatibe with human blood and can be used for in-vivo applications [Mehta et al., 2014].

Fig. 3.12 Optical image of hemolysis activity of SF-GG_b-SF after 1h incubation at 37°C with 2% blood in physiological saline, along with +ve (blood in water) and –ve (blood in saline) controls

b. Surface roughness

As the surface roughness is a crucial parameter for cell attachment, growth as well as migration thus rough surfaces claims better suitability for tissue growth [Lampin, et al., 1997]. The roughness of the surface was analyzed though AFM imaging (*Fig. 3.13 a-c*). The values of mean absolute roughness (Ra), root mean squire roughness (Rq) and of maximum peak height (Rz) for SF-GG_b-SF were found to be 37.5 nm, 54.1 nm and 222 nm respectively.

c. Dehydration rate or water evaporation rate (WER)

Rate of dehydration was evaluated through dehydration test. Dehydration profile was drawn as a function of percentage weight loss with time (*Fig 3.14*).

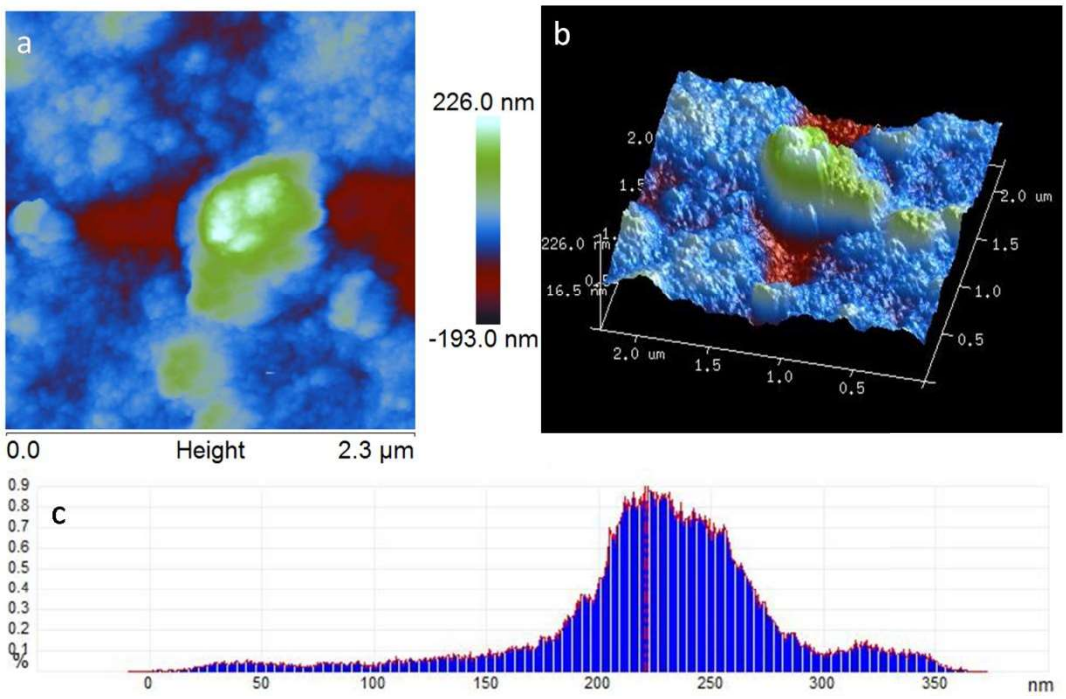

Fig 3.13 AFM image of the SF-GG$_b$-SF surface (a) 2D image, (b) 3D image (c) Height profile of the corresponding AFM image

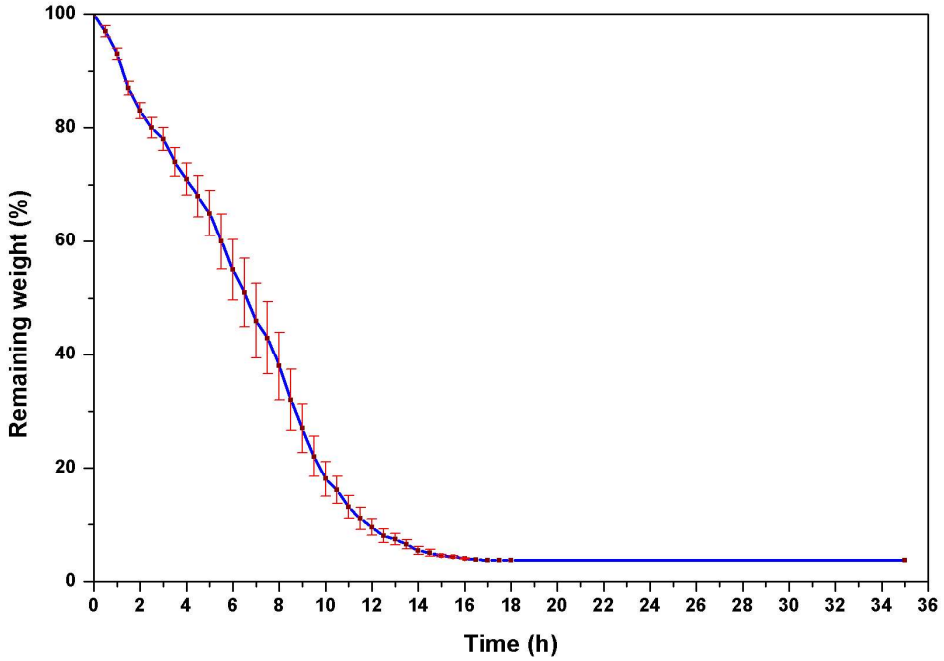

Fig 3.14 Rate of dehydration of SF-GG$_b$-SF at 37°C and 35% relative humidity

Swollen SF-GG_b-SF exhibit slow dehydration rate and take 16 h to completely dehydrate. The slow rate of dehydration is better for the material utilized to fabricate wound dressings and other biomaterials which are desired to provide moist environment at the site of application [Li et al., 2015].

d. FTIR analysis

FTIR spectrum of SF-GGb-SF was analyzed in the range of 4000-400 cm^{-1}(*Fig 3.15*).

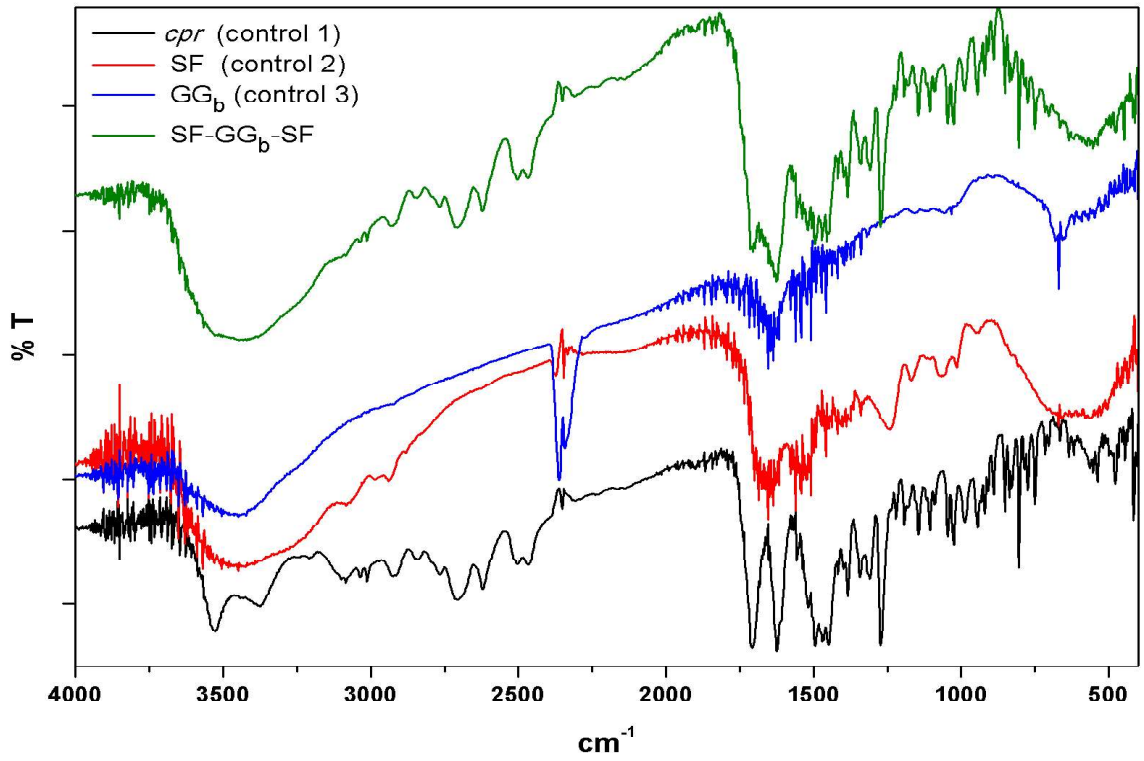

Fig. 3.15 FTIR spectra of SF-GG_b-SF along with SF_{sc}, GG_b and *cpr* as controls.

FTIR spectra SF_{sc}, GG_b and *cpr* was taken as control for comparison. FTIR spectra of SF_{sc} and GG_b showed many prominent bands. Broad band around 3400-3600 cm^{-1} in spectra of SF_{sc} and GG_b corresponds to –OH stretching [Bai and Abraham, 2002]. Bands in the range of 1600-1700 cm^{-1} represents amide I vibrations whereas the bands in the range of 1500–1600 cm^{-1} signifies the amide II vibrations. The amide I band mainly comes from C=O stretching along with the

minor contributions of N–H in-plane bending, whereas C–N stretching and N–H in-plane bending together arise amide II band [Ling et al., 2013]. Distinguished band at 1640 cm^{-1} represents the random coil whereas band at 1530 cm^{-1} represents β-sheet structure of SF [Ling et al., 2013]. Besides –OH stretching around 3400-3600 cm^{-1}, GG_b also shows a small band around 1057 cm^{-1} which represent C-O-C glycosidic linkage between its monomers [Coutinho et al., 2010]. IR spectra of *cpr* also showed many bands, main bands of *cpr* appears at 1705, 1623, 1460, 1274 and 1040 cm^{-1} which are assigned to C=O stretching vibration of carbonyl group of acid, δN-H bending of quinolines, -C-O- stretching vibration, δO-H bending and C-F stretching of fluride group respectively [Sahoo et al., 2012].

cpr loaded SF- GG_b-SF shows a wider band at 3500 to 3400 cm^{-1} which was assigned to O-H stretching vibration and hydrogen bonding. Bands between 3000 and 2600 cm^{-1} represented strong hydrogen bonding between drug and polymer [Sahoo et al., 2012]. Band of -C-O- stretching vibration of *cpr* showed a sifting from 1460 cm^{-1} and appears at 1454 cm^{-1} in IR spectra of SF-GG_b-SF which is also due to *cpr*-polymer interaction. From following signals and band pattern it can be concluded that *cpr* mainly intact with polymeric system in SF-GG_b-SF through intermolecular hydrogen bonding and some other interactions.

e. Antimicrobial activity

Finally, antibacterial behavior of SF-GG_b-SF against both *E. coli* and *S. aureus,* was evaluated through cell viability test. Antimicrobial effectivity of SF-GG_b-SF was investigated in two individual experiments conducted at different times to explore the variation in the antimicrobial potential of the scaffold with passage of time after application. First experiment was conducted with native scaffolds to know the effectiveness of the scaffold at the time of application. Whereas, the second experiment was conducted with the scaffold that was previously placed in SWF for 24 h to know the effectiveness of the scaffold after 24 h of application. *Fig. 3.16*

represent the experimental results of first set of experiments with native scaffold whereas *Fig. 3.17* represents the results of second set of experiments with pre incubated scaffold for 24h in SWF. In the first experiment, SF-GG_b-SF showed faster rate of inhibitory action on *E. coli* and *S. aureus* via killing 99.5% and 98.6% viable bacterial cells within 4h respectively. The initial strong antimicrobial effect was due to initial burst release of *cpr* from SF-GG_b-SF. In the second experiment, the rate killing of bacteria was drastically depleted and kills only 18.2% and 12.4% cells of *E. coli* and *S. aureus* in 16h. The reason behind this decreased antimicrobial effectivity was that during presoaking or pre incubation of SF-GG_b-SF in SWF for 24 causes the loss of most of the loaded *cpr* due to release and after 24 h of incubation the SF-GG_b-SF does not able to provide effective release of *cpr*. These findings are also in agreement with drug release studies which indicated that most of the *cpr* get released in initial 12h.

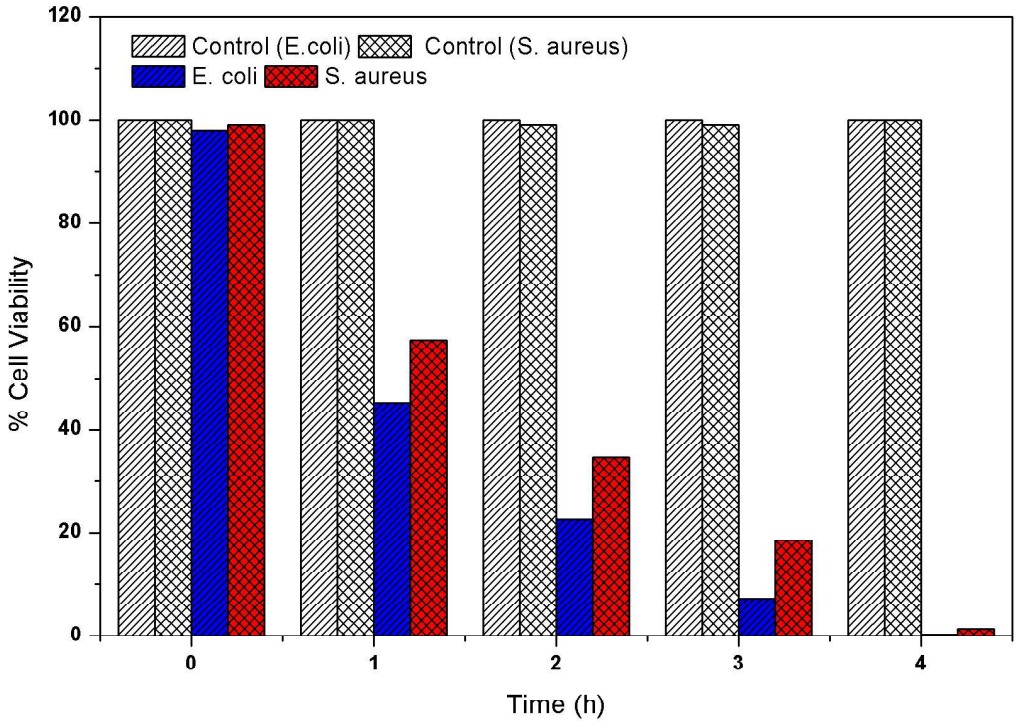

Fig. 3.16 Loss of cell viabilities of *E. coli* and *S. aureus* due to antimicrobial effect of SF-GG_b-SF in the first set of experiment conducted by native scaffold

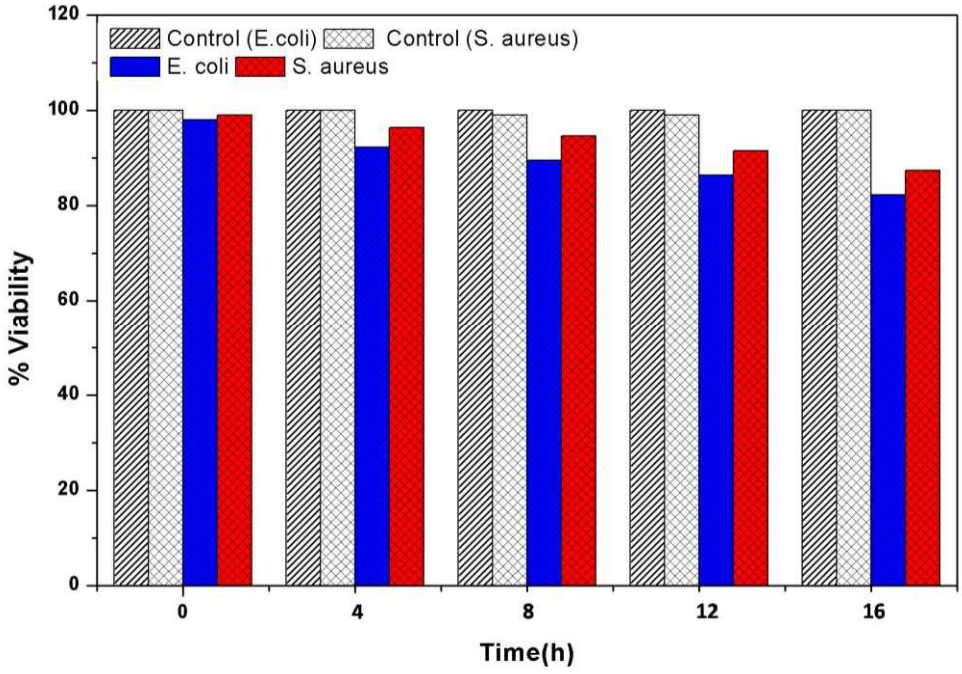

Fig. 3.17 Loss of cell viabilities of *E. coli* and *S. aureus* due to antimicrobial effect of SF-GG$_b$-SF in the second set of experiment conducted with the scaffold pre-incubated in SWF for 24h

3.5 Conclusion of the chapter

In this study it was found that SF$_{sc}$ poses excellent porosity and mechanical strength but poor swelling properties and drug loading capabilities. Blending of GG with SF improves the exudates absorption capacity and drug loading capacities of SF but porosity and mechanical strength get depleted. Interestingly, SF-GG$_b$-SF also showed improved swelling properties and drug loading capacities without compromising with porosity and mechanical strength up to larger extent. SF-GG$_b$-SF releases the *cpr* in a more sustained manner for longer period of time (12h) as compare to SF-GG (6h). Kinetic studies illustrated that sustained release of *cpr* from SF-GG$_b$-SF takes place through anomalous (Non-Fickian) diffusion by following 'Korsmeyer-Peppas kinetic model' with R^2 0.976. SF-GG$_b$-SF showed excellent

haemocompatibility for human blood with only 3.7% of hemolysis. Mean absolute roughness (Ra) of the scaffold surface was 37.5 nm. Real time antimicrobial assessment of SF-GG_b-SF via cell viability test has proven initially SF-GG_b-SF showed strong antimicrobial effect but after 24h of incubation in SWF its antimicrobial potential drastically depletes.

Thus it seems that making hybrid scaffold with entrapped gellan gum bead can be a superior option over approach of blending of both polymers together. But still SF-GG_b-SF could not be considered as ideal biomimmic scaffolds because in this system the main porous matrix is composed of SF component that is only protein part. For ECM biomimmic it is desirable that the surface should be made up of both protein and carbohydrate components [Bhardwaj et al., 2011; Teimouria et al., 2015; Wenk et al., 2011]. Although the surface of SF-GG is composed of both protein and carbohydrate components but in this case poor porosity limits its ideality. Moreover the degradation rates of both types of scaffolds are very poor in SWF, which is undesirable. Furthermore, the drug release is only continues up to 6h and 12h in case of SF-GG and SF-GG_b-SF respectively. This short release period can only provide initial antimicrobial effect up to short duration and scaffolds will not be capable of providing the antimicrobial support for prolonged period of time. Surface roughness (Ra; 37.5 nm) was also not close enough to the roughness index of native ECM (Ra; 157 nm) [Anderson et al., 2006].

Due to these shortcomings it is necessary to further improve the designed scaffolds. For this purpose, we modified our scaffolds by replacing gellan gum with chitosan and to provide the prolonged antimicrobial activity we incorporated

additional antimicrobial agent i.e. silver nanoparticles along with *cpr.* For economic feasibility and eco-friendly approach we decided to synthesize the silver nanoparticles through green route. Next two chapters of the thesis are dedicated to the green synthesis of nanoparticles and last chapter is about designing of modified scaffolds and its in-vivo evaluation.